BIOCHEMISTRY
including biophysical chemistry & molecular biology

Article

pubs.acs.org/biochemistry

Quantitative Analysis of the Effects of Photoswitchable Distance Constraints on the Structure of a Globular Protein

Andrew A. Beharry,[†] Tao Chen,[‡,§] M. Sameer Al-Abdul-Wahid,[∥] Subhas Samanta,[†] Kirill Davidov,[†] Oleg Sadovski,[†] Ahmed M. Ali,[†] Simon B. Chen,[†] R. Scott Prosser,[∥] Hue Sun Chan,*[,‡,§] and G. Andrew Woolley*[,†]

[†]Department of Chemistry, University of Toronto, 80 Saint George Street, Toronto, Ontario M5S 3H6, Canada

[‡]Department of Biochemistry and Department of Molecular Genetics, University of Toronto, 1 King's College Circle, Toronto, Ontario M5S 1A8, Canada

[§]Department of Physics, University of Toronto, 60 Saint George Street, Toronto, Ontario M5S 1A7, Canada

[∥]Department of Chemistry, University of Toronto at Mississauga, 3359 Mississauga Road North, Mississauga, Ontario L5L 1C6, Canada

Supporting Information

ABSTRACT: Photoswitchable distance constraints in the form of photoisomerizable chemical cross-links offer a general approach to the design of reversibly photocontrolled proteins. To apply these effectively, however, one must have guidelines for the choice of cross-linker structure and cross-linker attachment sites. Here we investigate the effects of varying cross-linker structure on the photocontrol of folding of the Fyn SH3 domain, a well-studied model protein. We develop a theoretical framework based on an explicit-chain model of protein folding, modified to include detailed model linkers, that allows prediction of the effect of a given linker on the free energy of folding of a protein. Using this framework, we were able to quantitatively explain the experimental result that a longer, but somewhat flexible, cross-linker is less destabilizing to the folded state than a shorter more rigid cross-linker. The models also suggest how misfolded states may be generated by cross-linking, providing a rationale for altered dynamics seen in nuclear magnetic resonance analyses of these proteins. The theoretical framework is readily portable to any protein of known folded state structure and thus can be used to guide the design of photoswitchable proteins generally.

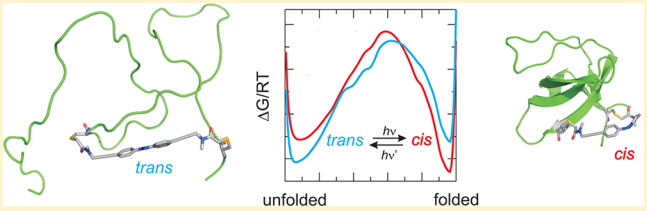

Light-sensitive proteins offer exciting prospects for external manipulation and probing of complex biochemical systems.[1−3] A number of mechanisms for photocontrol of protein function are possible, such as control of a tethered inhibitor[4] or reorganization of key side chains at an active site.[5] However, such strategies are protein specific and must be approached on a case by case basis. A general approach to optical control that could be applied to a wide range of potential target proteins would be very desirable. We expect that photocontrolling a protein could be accomplished in a general manner by unfolding, i.e., disrupting all or most native folded state contacts, using intramolecular photoswitchable cross-links. Although this approach still requires knowledge of the folded state structure, an effective photoswitchable cross-link could presumably be applied to all proteins with a similar fold.

Photocleavable cross-links have been used to hold proteins in an unfolded, inactive state by forcing together sites not normally close in the native folded structure.[6,7] Irradiation can then restore the active state.[8−12] Such systems are irreversible, however, and so cannot be used to produce complex or repeating patterns of biomolecule activation (e.g., refs 4 and 13). In a reversible system, the choice of cross-linking site is more complicated because the cross-link must disrupt folding in one isomeric state but must be compatible with biomolecule function (it must not sterically occlude a binding site, for instance) in the other isomeric state.

Reversible formation and disruption of simpler elements of protein structure, such as α-helices and β-hairpins, by photoswitchable cross-links have been studied quite extensively. Azobenzene-based photoswitches can be designed so that the *cis* isomer has an end-to-end distance that matches the distance between two ends of a β hairpin structure whereas the *trans* isomer is too long to permit a normal hairpin to form.[14−16] Likewise, the effects of azobenzene-based cross-linkers on peptide helix content can be predicted by comparing the length of the linker with the distances between attachment points in the intrinsic conformational ensemble (α-helix/random coil) of the peptide.[17,18]

In contrast to regular secondary structures, globular proteins provide a much wider choice of possible attachment sites for a

Received: May 24, 2012
Published: July 17, 2012

   dx.doi.org/10.1021/bi300685a | *Biochemistry* 2012, 51, 6421−6431

cross-linker and it is not clear a priori how introducing a specific type of distance constraint at a particular site will alter the stability of the native folded state; thus, it is unclear how to choose which site and which cross-linker to use for photocontrol.

Previously, we reported the introduction of the azobenzene-based cross-linker BSBCA [3,3′-bis(sulfonato)-4,4′-bis(chloroacetamide) azobenzene (**1**)] between Cys residues at positions 3 and 29 (L3C and L29C) of a mutant Fyn SH3 domain.[19] This pair of attachment sites was chosen to be compatible with the *cis* form of the cross-linker, but too close together to be compatible with the *trans* form.[20] Also, cross-linking at this site is unlikely to sterically interfere with ligand binding. We found that the *cis* form of BSBCA stabilized the folded state, and the *trans* form destabilized the protein. However, the extent of destabilization was such that approximately 50% folded and 50% unfolded conformations coexisted in slow exchange in the *trans* (dark-adapted) state as judged by a qualitative examination of $^{1}H-^{15}N$ HSQC spectra.[19] Thus, while optical control of global folding and unfolding was seen with this system, the degree of photocontrol is probably insufficient to allow effective photocontrol of function in an in vivo setting.[13,21]

On the basis of this result, we synthesized a second photoswitchable cross-linker that, in its *trans* form, exhibited a longer end-to-end distance. Our expectation was that this cross-linker would cause a greater degree of destabilization of the native folded state in the dark. The first part of this report describes experimental work that characterizes the effects of this linker on the Fyn SH3 domain. Contrary to expectation, the longer linker appears to cause less destabilization of the folded state than the short linker.

In an attempt to understand this experimental observation in quantitative terms, we developed a theoretical model of these photoswitchable proteins. For our purpose, a thermodynamically rigorous model that can reliably sample folded and unfolded states is required. In general, polymer theory predicts that the unfolded state is destabilized, thus the folded state is stabilized, by an intramolecular cross-link because of a reduction in conformational entropy and the extent of destabilization varies approximately as a function of the logarithm of the number of residues that lie in the loop closed by the cross-link, longer loops being more destabilizing.[22−24] Here, however, we are more interested in how a cross-link at a particular site can destabilize the folded state. This must depend on the actual structure of the cross-link and the nonrandom conformational distribution of the protein, but these features are difficult to capture by analytic polymer theory. Explicit-chain models[25] are needed to address their effects.[26]

Several explicit-chain models have been developed recently for cross-linked peptides and proteins. These include a Cα Gō model[26] and an all-atom model with a knowledge-based transferrable potential[27] that were used to analyze the effect of cross-linking on the behavior of short peptides of ∼20 residues, a CHARMM molecular dynamics simulation of the kinetics of helix formation in a 16-residue peptide with a photoswitchable cross-link,[28] and an AMBER molecular dynamics unfolding simulation of two interlinked protein domains of 76 and 110 residues that exhibit an antagonistic folding−unfolding equilibrium.[29] In contrast, our investigation entails simulating many folding−unfolding cycles for proteins with ∼60 residues, a task that cannot be achieved using all-atom models with current computing resources. Moreover, for new linker designs, it would not be clear a priori what folding and unfolding rates would occur in practice, and so what time frame of simulation would be required. For these reasons, we opted to use computationally tractable coarse-grained native-centric Gō models[30−34] modified to explicitly include a cross-linker of a given shape and flexibility.

Gō models are based on the dominant role of native topology and have provided valuable insights into the general principles of protein folding.[25,30,31,35] One limitation of Gō models is that they do not include favorable nonnative interactions unless they are augmented with sequence-dependent terms.[36−38] For instance, Gō models did not predict the stabilization of a misfolded state by an intramolecular cross-link in a study of peptide helices.[27] Our main concern, however, is the general manner in which a cross-link can effectively disrupt native contacts. As reported below, as a first approximation, appropriately modified native-centric Gō models can successfully rationalize the experimentally observed extent of destabilization by cross-linkers of different designs and thus afford general guidelines for the photocontrol of protein structure.

RESULTS AND DISCUSSION

Azobenzene exhibits robust, reversible *cis*−*trans* isomerization about the N═N double bond.[39] The *trans* conformation of azobenzene is ∼10−12 kcal/mol more stable than the *cis* conformation,[40] and the thermal barrier to the interconversion of *cis* and *trans* isomers is ∼18 kcal/mol.[17] These values should be more than sufficient to drive substantial conformational change in proteins where typical folding free energies are between 5 and 15 kcal/mol.[41] In general, one can produce ∼100% of the *trans* isomer by thermal relaxation and ∼60−90% of the *cis* isomer by photoirradiation. Thus, it is possible to change the *cis* content of an azobenzene-modified target by a greater fraction than the *trans* content. For this reason, we design systems so that the *cis* isomeric state of the cross-linker is associated with the active, folded state of the protein.

The 59-residue Fyn SH3 domain, a well-studied model protein[36,42,43] with hundreds of related folded domains,[44] was mutated to introduce Cys residues at positions 3 and 29 (Figure 1). The cross-linker studied previously [BSBCA (**1**)] as well as a longer cross-link, the alkyne derivative (**2**), were synthesized and used to cross-link these sites (Figure 1) (see the Supporting Information). To characterize the lengths of the isolated cross-linkers, all-atom molecular dynamics simulations were performed as described previously (Figure 1) (see the Supporting Information).[45,46] Whereas in their *cis* states both cross-linkers can adopt conformations that are fully compatible with the folded state (∼10.8 Å between Cα atoms), their *trans* states differ substantially with alkyne-containing linker **2** showing a broader distribution of end-to-end distances and a significantly longer mean length than linker **1**. Because the *trans* form of **2** has a longer end-to-end distance, we expected it might produce greater destabilization of the folded state.

Experimental Determination of Protein Folded/Unfolded State Stability. The Fyn SH3 domain with L3C and L29C mutations was first characterized by NMR spectroscopy. Figure 2 shows ^{15}NH HSQC spectra of the un-cross-linked protein and the *trans* forms (dark-adapted states) of the protein with cross-linkers **1** and **2**. Whereas the un-cross-linked protein gives a well-resolved spectrum similar to that of the wild-type protein,[43] the cross-linkers cause major changes. Cross-linker **1**

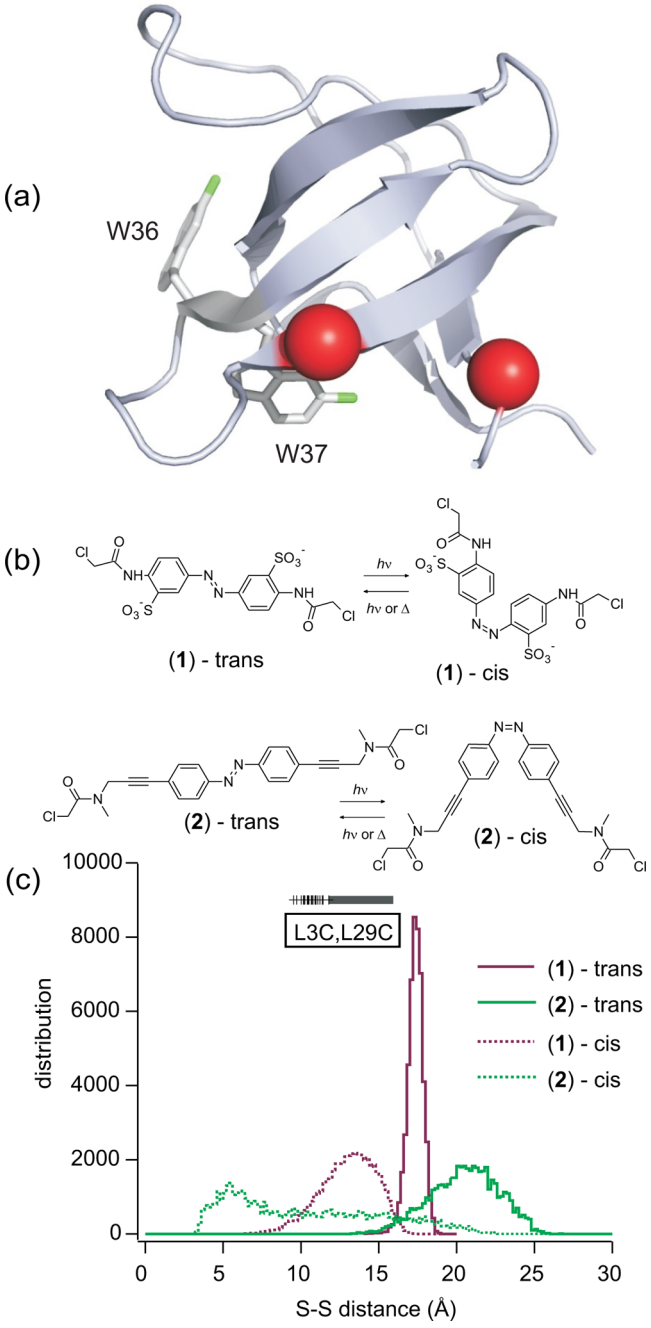

Figure 1. (a) Fyn SH3 domain (PDB entry 1SHF) showing the Cα atoms of residues 3 and 29 (L3C and L29C) as red spheres. The cross-linker links these sites. The two 5-F-Trp residues used as reporters for folded and unfolded states are shown as sticks with the fluorine atoms colored green. (b) Structures of the cross-linkers used in this study. (c) Histograms showing the sulfur-to-sulfur distance distributions of the isolated cross-linkers. The Cα−Cα distances are shown in panels c and f of Figure 5 and have a broader distribution in each case, as expected because extra flexible bonds are included. The sulfur-to-sulfur distances are shown here to conform to previously published conventions.[19] The distances between side-chain γ atoms observed in X-ray (PDB entry 1SHF) (thick horizontal line) and NMR (PDB entry 1A0N) (crosses) structures of the Fyn SH3 domain are also shown at the top of panel c.

produces a spectrum with approximately double the number of peaks, although many are poorly resolved in the center of the spectrum. As with the L3C/L29C/T47A Fyn SH3 cross-linked species studied previously,[19] this doubling of the total number of peaks indicates the coexistence of a relatively normally folded species (as judged by the superposition of one set of cross-peaks with those in the spectrum of the un-cross-linked protein) and a globally unfolded state characterized by a cluster of peaks with a small range of chemical shifts between 8.0 and 8.5 ppm on the proton axis.[19,43] Introducing alkyne derivative **2** also causes a global change in the spectrum with a loss of dispersion and an increase in the number and intensity of peaks in the center of the spectrum, but overall, there is a decrease in the total number of peaks and there are large variations in peak intensity.

Irradiation with UV light (365 nm) to produce ~65% *cis*/35% *trans* efficiently repopulated the folded state of the protein in each case. Figure S3 of the Supporting Information shows resonances that increase in intensity upon UV exposure of the cross-linked proteins. These peaks correspond closely in chemical shift to those of the folded state (except near the attachment point of the cross-linker) (Figure S3). Those that decrease in intensity upon UV exposure correspond to unfolded states. Thus, photocontrol of global folding and unfolding is occurring with both cross-linkers. We then wished to quantitatively assess the degree of photocontrol, i.e., the degree to which the protein was unfolded by the *trans* forms of the linkers.

Although, at first glance, the HSQC spectrum of the dark-adapted *trans* form of the alkyne **2**-linked protein seems to indicate a greater fraction of unfolded protein than with cross-linker **1** (Figure 2b,c), a closer inspection indicates that strong signals characteristic of the folded state persist. This can be seen clearly by examining the indole NH region of the HSQC spectra (Figure 3). The Fyn SH3 domain has two Trp residues, W36 and W37. Although these are adjacent in the primary sequence, they occupy sites with very distinct environments in the three-dimensional structure where W36 is considerably more solvent exposed (as calculated using Surface Racer[47]) than W37 (Figure 1). In the folded, un-cross-linked protein, the Trp indole NH signals appear as two well-resolved peaks in the HSQC spectrum (Figure 3 and Supporting Information). In the unfolded state, they occur as two very closely spaced peaks at 20 °C. As the temperature is increased, the intensity of the folded state signals decreases, the intensity of the unfolded state signals increases, and the two unfolded peaks merge into one. A ZZ-exchange experiment performed on the un-cross-linked protein further establishes the assignment of signals to the folded and unfolded states (Figure 3c).

The corresponding regions of the dark-adapted *trans* **1** and **2**-cross-linked species are shown in panels d and e of Figure 3, respectively. Whereas the *trans* **1**-cross-linked species shows four peaks (labeled f_1, f_2, u_1, and u_2) consistent with the slow exchange of a folded state with resolved Trp indoles and an unfolded state with poorly resolved Trp indoles, for the alkyne **2**-linked species, four peaks are also seen, but these are identified as one intense (merged) unfolded signal and three distinct folded Trp signals [one intense (f_1) and two weaker (f_2 and f_3)]. This assignment is confirmed by the behavior of these peaks as a function of temperature (Figure S6 of the Supporting Information) and by a ZZ-exchange experiment (Figure 3f) that clearly shows exchange between f_2 and f_3, as well as between f_1 and the unfolded state signal and f_2 and the unfolded state signal. The presence of the extra folded state cross-peak indicates that the linker has stabilized a distinct (misfolded) conformation such that one Trp residue can sample two environments (f_2 and f_3). Exchange between

dx.doi.org/10.1021/bi300685a | *Biochemistry* 2012, 51, 6421−6431

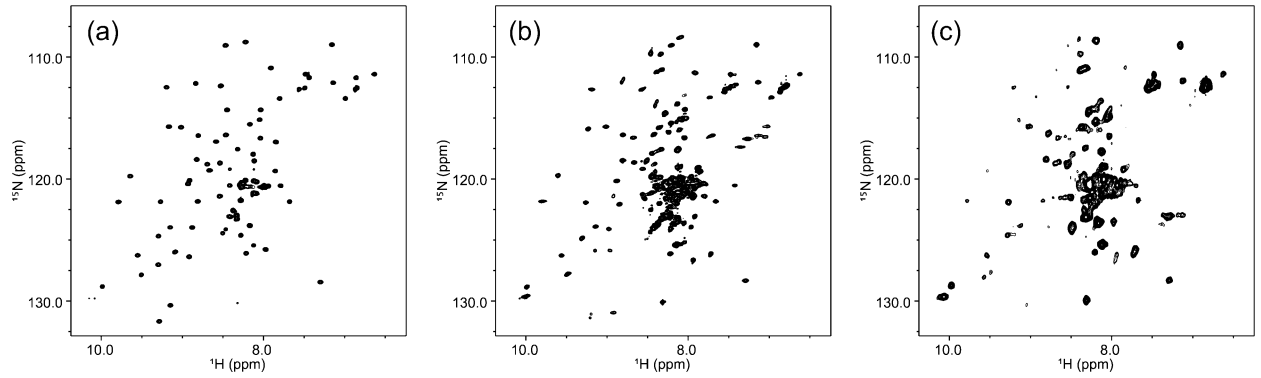

Figure 2. ^{15}NH HSQC spectra. (a) Un-cross-linked L3C/L29C Fyn SH3, (b) dark-adapted (*trans*) **1**-cross-linked L3C/L29C Fyn SH3, and (c) dark-adapted (*trans*) **2**-cross-linked L3C/L29C Fyn SH3, all at 20 °C.

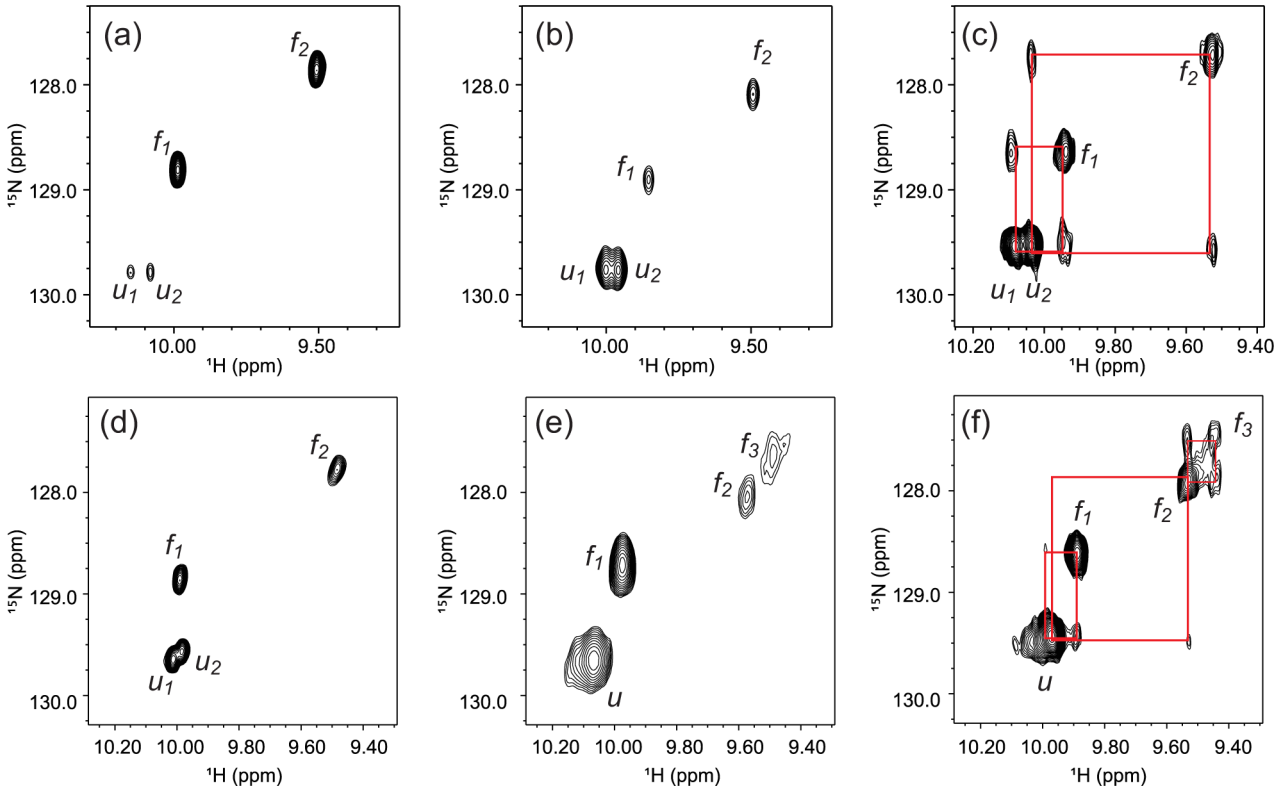

Figure 3. (a) Sections of the HSQC spectra of un-cross-linked L3C/L29C Fyn SH3 at 20 °C showing the two Trp indole NH resonances. The folded state predominates. (b) The same section at 50 °C, where the unfolded state predominates. (c) ZZ-exchange experiment with un-cross-linked Fyn SH3. (d) Trp indole NH region of the HSQC spectrum of **1**-cross-linked L3C/L29C Fyn SH3 in the dark-adapted (*trans*) form at 20 °C. (e) Trp indole NH region of the HSQC spectrum of **2**-cross-linked L3C/L29C Fyn SH3 in the dark-adapted (*trans*) form at 20 °C. (f) ZZ-exchange experiment with dark-adapted **2**-cross-linked L3C/L29C Fyn SH3 at 40 °C.

folded and misfolded states and altered dynamics can result in signal intensity being lost during the INEPT transfer times of the HSQC experiment. This explains why the HSQC spectrum of the alkyne **2**-linked species has fewer signals overall and shows wide variations between the intensities of different peaks compared to the spectra for un-cross-linked protein or the **1**-linked species. It should be noted that while such a misfolded state has a contact pattern that differs from that of the un-cross-linked native structure, it does not necessarily contain stable nonnative contacts.

Although the HSQC spectra provide a qualitative indication of the global nature of the folding or unfolding response, it is difficult to accurately assess relative populations through ratios of peak intensities, both because of significant line broadening due to conformational exchange and because of the INEPT transfer periods in the pulse sequence, which tend to filter out broader components. A one-dimensional ^{19}F NMR experiment instead allows populations to be more reliably determined from ratios of areas associated with peaks of interest. Moreover, ^{19}F NMR chemical shifts tend to be quite sensitive to unique states (environments).

For the un-cross-linked protein, the behavior seen in the Trp indole HSQC spectra is reflected in the ^{19}F spectra. Two peaks are observed to decrease in intensity, while one peak increases in intensity as the temperature is increased (Figure 4a). At 20 °C, the ratio of the areas under the folded and unfolded peaks is ~12:1, indicating the [^{19}F]Trp-modified protein has a free energy of folding of ~1.5 kcal/mol under these conditions

dx.doi.org/10.1021/bi300685a | *Biochemistry* 2012, 51, 6421−6431

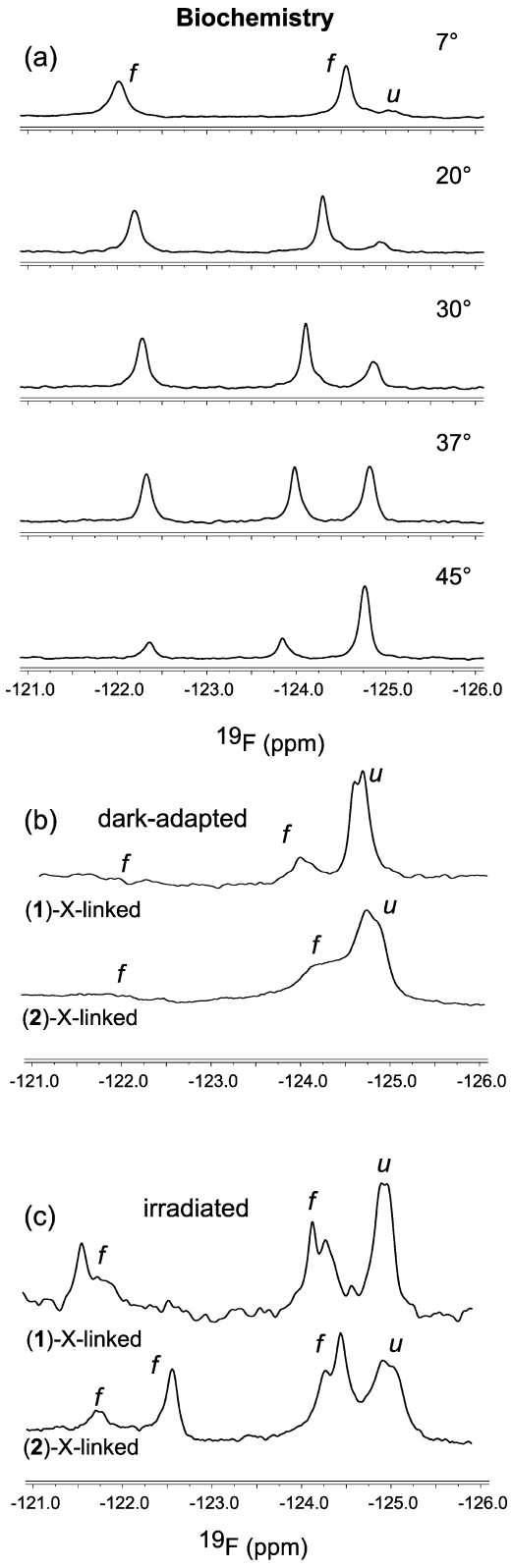

Figure 4. (a) ^{19}F NMR spectra of 5-F-Trp-labeled L3C/L29C Fyn SH3 at a series of temperatures showing the decrease in intensity of the folded state as the temperature increases. (b) ^{19}F NMR spectra of 5-F-Trp-labeled cross-linked L3C/L29C Fyn SH3 at 20 °C under dark-adapted conditions. (c) Like panel b but after UV irradiation (365 nm) (see the Supporting Information).

($\Delta G/k_BT = -2.4$, where ΔG is the free energy of folding, k_B is the Boltzmann constant, and T is the absolute temperature).

The ^{19}F spectra of the cross-linked proteins in the dark-adapted (*trans*) state (Figure 4b) reflect the dynamics suggested by the HSQC spectra with the peaks for the **2**-cross-linked species significantly broader than for the **1**-cross-linked species. In the dark state of each species, only one folded Trp signal is evident, although very broad signals are seen near the position of the second folded Trp signal in the un-cross-linked protein (Figure 4b).

Upon irradiation, all the folded Trp signals are recovered (Figure 4c), but even here, the alkyne **2**-modified protein has an extra signal from a folded Trp indicating the existence of an extra misfolded conformation. If we take the integrated areas under the ^{19}F peaks to represent populations of folded or unfolded states as indicated (Figure 4b), the extent of destabilization of the folded state by the cross-linkers can be calculated (Table 1). We note that if we take the Trp indole peak volumes from the HSQC spectra for the more mobile (presumably surface exposed) Trp only (Figure 3a,d,e), we obtain a similar result. These data indicate that the *cis* isomers of the cross-linkers produce ~100% folded state because the fraction folded is the same as the fraction *cis* produced by irradiation (Table 1). These data also indicate that, contrary to expectation, the *trans* form of the longer alkyne (**2**) cross-linker produces less destabilization of the folded state than the short linker (**1**).

Table 1. Characterization of 1- and 2-Linked Protein

protein	fraction folded (*trans*)	$\Delta G/k_BT$ (*trans*)	$\Delta G/k_BT$ (*trans*)	predicted $\Delta G/k_BT$ (relative to un-cross-linked)[a]	fraction folded (irradiated)[b]
un-cross-linked	0.92	−2.4	0	0.0	0.92
1-cross-linked	0.16	1.7	4.1	3.6	0.6
2-cross-linked	0.5	0	2.4	1.2	0.67

[a]See the text for details. [b]Not corrected for % *cis*.

Theoretical Modeling of Protein Folded/Unfolded State Stability. Aiming to understand these results, we performed simulations of the folding of the Fyn SH3 domain using a native-centric Gō-type coarse-grained explicit-chain model[30−34] with desolvation barriers.[34,48−50] SH3 domains have been studied computationally using a variety of coarse-grained chain models (e.g., refs 33, 36, 38, 51, and 52). Here, thermodynamic sampling of conformational distributions was conducted using Langevin dynamics in conjunction with umbrella sampling and replica exchange techniques[53−55] with the same model parameters that were used by Liu and Chan[48] as described in the Supporting Information.

In the models, a simplified linker was introduced between the Cα atoms of residue positions 3 and 29. The representation of this was a bar with a single joint (for the *cis* from) or two joints (for the *trans* form) that exhibits a mean end-to-end distance $\langle r \rangle$ and a flexibility σ [standard deviation of r, governed by the spring constants k_θ for the joints (see Figure 5)]. Further details of the construction of the model linker are provided in the Supporting Information. Via adjustment of the mean length and the spring constants of the joints in the models, distance distribution histograms approximately matching the ones obtained from all-atom MD simulations of the experimental linkers could be obtained. For example, Figure 5c shows the

dx.doi.org/10.1021/bi300685a | *Biochemistry* 2012, 51, 6421−6431

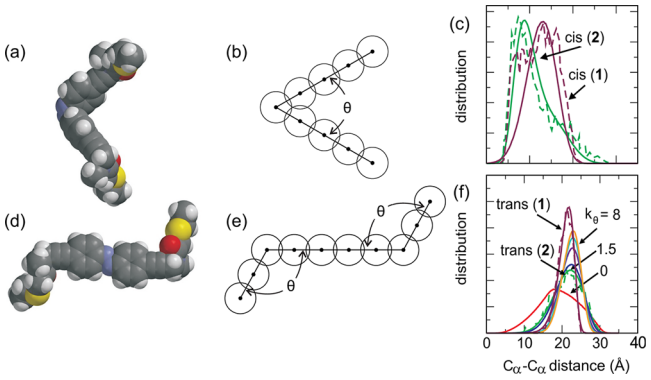

Figure 5. Modeling the cross-linkers. (a) Space-filling model of the *cis* form of the alkyne **2** cross-linker generated using Spartan. (b) General structure of the model *cis* linkers. Each circle represents an excluded-volume repulsion term $(2.8\ \text{Å}/r)^{12}$, where r is the distance, in angstroms, between the center of the circle and any Cα position in the model protein. The main degree of freedom is the angle θ subtended by the two straight branches. Variation of θ is harmonic for the short *cis* linker and is anharmonic for the long *cis* linker (see the Supporting Information for further details). (c) Normalized end-to-end distance distributions of free *cis* linkers (not attached to the protein). Distributions for the short (**1**) and long (**2**) model *cis* linkers are plotted as the solid purple and green curves, respectively. Included for comparison (dashed curves) are the Cα−Cα distance distributions determined by MD simulation for the same linkers (calculated as in Figure 1). (d) Space-filling model of the *trans* form of the alkyne **2** cross-linker generated using Spartan. (e) General structure of the model *trans* linker. Variation of θ is harmonic; different linker properties can be obtained by varying the equilibrium angle θ_0 and the associated spring constant k_θ. (f) Normalized end-to-end distance distributions of free *trans* linkers. Distributions (solid curves) are shown for $\theta_0 = 104.5°$ and k_θ = 0, 1.5, 2.0, 4.0, 6.0, and 8.0, which are plotted as red, green, dark blue, purple, light blue, and orange lines, respectively. Included for comparison (dashed green curve) is the Cα−Cα distance distribution determined by MD simulation for the alkyne **2** *trans* linker. A similar procedure was used to simulate the short linker **1** (purple).

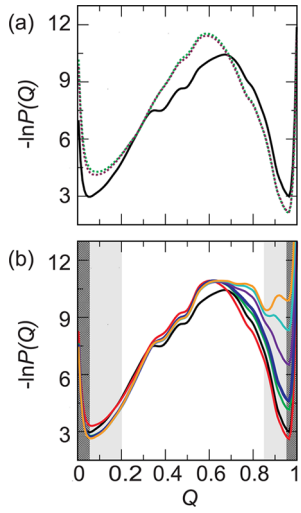

Figure 6. Effects of linkers on the folding landscape in the explicit-chain folding/unfolding model. All free energy profiles were simulated at the same temperature (T = 0.87 in model units), which is approximately the transition midpoint of the WT protein in our model. $P(Q)$ is the normalized distribution of conformational population as a function of Q; $P(Q)$ and $-\ln[P(Q)]$ were determined by the Langevin dynamics sampling procedure described in the Supporting Information. The WT free energy profile is shown in black in both panels. (a) For *cis* linkers, free energy profiles of the model protein with the short and long model *cis* linkers in Figure 5c are plotted in purple and green, respectively. The shifts of these profiles relative to that for the WT (black) indicate that the folded state of the model protein is stabilized by the *cis* linkers. (b) For *trans* linkers, free energy profiles of the model protein with the *trans* linkers in Figure 5e are plotted using the same color code as that in Figure 5f. The dark-shaded regimes ($Q < 0.06$ and $Q > 0.95$) define the folded state stability $\Delta G/k_BT$ in this study. The light-shaded regimes ($0.06 \le Q < 0.2$ and $0.95 \ge Q > 0.85$) are used for broader sampling of open and collapsed conformations.

distributions for *cis* models of the BSBCA cross-linker (**1**) and the alkyne cross-linker (**2**) with corresponding MD-derived histograms. Figure 5f shows corresponding plots for the *trans* forms of the BSBCA cross-linker (**1**) and the alkyne cross-linker (**2**). In addition, simulations with models of the *trans* alkyne cross-linker (**2**) (with $\langle r\rangle$ = 22 Å) and a range of k_θ values are shown. These models were used to systematically explore the role of linker flexibility in protein destabilization. The order parameter Q, representing the fraction of native contacts, was used to judge the degree of folding of the protein models.[31,34,55] Plots of free energy as a function of Q for a series of model linkers are given in Figure 6.

The *cis* cross-linkers promote folding as judged by the favorable change in ΔG (Figure 6a). They destabilize the unfolded state as expected. This effect does not appear to depend much on the details of the end-to-end distribution of the *cis* linker because the short (**1**) and long (**2**) species gave equivalent effects despite having different distributions. The effect of the *trans* form of the cross-linker on protein stability was more complicated. Figure 6b shows free energy profiles in Q space for a cross-linker with a mean length of ∼22 Å (like alkyne linker **2**) and varying flexibility. As the k_θ value increases, the linker becomes more rigid. As the rigidity of the cross-linker increases, larger and larger degrees of destabilization occur. There is interplay between the average end-to-end length $\langle r\rangle$ and flexibility in a cross-linker's ability to destabilize the folded state. We explored this by running simulations for a series of $\langle r\rangle$ and σ values. The result is shown in Figure 7. It is clear that destabilization of the folded state caused by an increase in the mean length of the linker can be nullified by an increase in the flexibility of the linker.

Using analogous simulations, we calculated the free energy change expected for model linkers specifically designed to mimic the short (**1**) and long (**2**) species in *trans* states (i.e., having the distance distributions as shown in Figure 5f). As in previous modeling studies,[31,34] the free energy of folding $\Delta G/k_BT = -\ln[P(\{Q\}_N)/P(\{Q\}_D)]$ was determined by the ratio between the native state population $P(\{Q\}_N)$ and the denatured state population $P(\{Q\}_D)$. These populations correspond to those in a narrow range of Q values around the native and denatured free energy minima, respectively. Model $\Delta G/k_BT$ values were determined predominantly by the relative populations at the native and denatured minima and were largely insensitive to the choice of the narrow range of Q values in its definition. The ranges for $\{Q\}_N$ and $\{Q\}_D$ that we used for this study are shown in Figure 6 (see further discussion in the Supporting Information). The predicted free energies of destabilization are given by the $\Delta G/k_BT$ value computed in the presence of a linker minus the $\Delta G/k_BT$ value computed without the linker. These free energy differences are included in Table 1 as "predicted $\Delta G/k_BT$ (relative to Un-X)" alongside the experimentally determined numbers from the ^{19}F NMR

dx.doi.org/10.1021/bi300685a | *Biochemistry* 2012, 51, 6421−6431

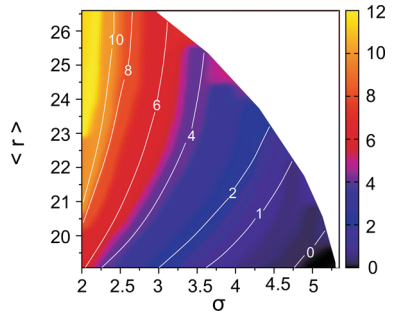

Figure 7. Effect of *trans* linker stiffness on folding stability. The contour plot shows folding stability $\Delta G/k_BT$ as a function of the average end-to-end distance, $\langle r \rangle$, and the standard deviation σ, of an extended class of model *trans* linkers we obtained by varying both k_θ and θ_0 in the basic setup described in Figure 5 (note that θ_0 is not restricted to 104.5° in this figure). The allowed region of $\langle r \rangle - \sigma$ variation is bounded on the right by data points for $\theta_0 = 180°$. All $\Delta G/k_BT$ values were calculated at the same model temperature as that used for Figure 6. The folding stability of the model WT protein (not cross-linked) at this simulation temperature is ≈0.4.

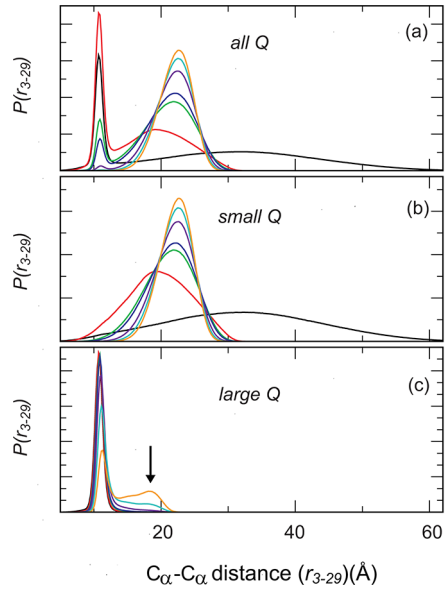

Figure 8. Effects of linker constraints on intraprotein Cα−Cα distance distributions. The distribution, $P(r_{3-29})$, of the distance r_{3-29} between Cα positions 3 and 29 was computed in the presence of a model *trans* linker attached to these positions. Results are shown for the class of model *trans* linkers in Figure 5f (same color code for the curves). The corresponding distributions for the WT protein (not cross-linked) are included for comparison (black lines). The distributions were sampled in three different conformational ensembles, encompassing (a) all conformations, (b) open conformations with $Q < 0.2$, corresponding to those in the low-Q shaded regime in Figure 6b, and (c) compact, nearly folded, and folded conformations with $Q > 0.85$, corresponding to those in the high-Q shaded regime in Figure 6b. The arrow in panel c highlights a nonnative distribution peak. This feature suggests that a *trans* linker can promote the formation of a compact, near-native, yet partially unfolded/misfolded state.

data given above. The theory confirms the experimental result that the *trans* form of **2** is less effective at destabilizing the folded state than the *trans* form of **1** despite having a longer mean end-to-end distance.

To explore the detailed origins of this result further, we examined the actual distances between linker attachment sites (r_{3-29}) in simulations of cross-linked proteins with linkers of different flexibility. These data are shown in Figure 8a. There is a significant tendency (because of the favorable free energy of folding of the native un-cross-linked protein) for the protein to drive the cross-linker to a distance matching that of the folded state, where Q is close to 1. Indeed, this effect is promoted because by restricting the conformational space of the unfolded state, cross-linkers favor folding. In the experimental systems, distance distributions of free cross-linkers (e.g., Figures 1 and 5) are generated by rotations about single chemical bonds so that even distances at the extreme ends of the distribution are not prevented by hard restraints such as bond lengths or steric clashes; they are only statistically unlikely conformations of the free linker. Thus, if the flexibility of a cross-linker allows an r_{3-29} value near the folded state, the protein will tend to select these conformations of the linker. For example, as seen in Figures 6 and 8, a very flexible cross-linker with a mean length of ∼20 Å actually promotes folding despite having a mean length that is approximately twice the distance between the Cα atoms in the folded state (red curve in Figures 6b and 8a).

It is, therefore, not the mean length of the linker that is critical for photocontrol, but the availability of linker conformations that are compatible with the folded state. Specifically, it is the ln(population) of the free linker (not the population itself) at the native separation that is important for determining native stability. −ln(population) is effectively an energy that must be added to the native-centric energy to evaluate the combined effect on protein stability. A logarithmic plot of the end-to-end distance distributions (Figure 9a) of the free short (**1**) and long (**2**) linkers clearly shows the long linker has a greater ln(population) at the critical distance.

For the series of model linkers with increasing stiffness values (Figure 5f), one can examine the free energy difference [difference in −ln(population)] of the linker between the folded state distance (10.8 Å) and the −ln(population) minimum, i.e., peak (P_{max}) of the population distribution (Figure S13 of the Supporting Information). This free energy difference correlates well with the free energy of destabilization seen when the linker is connected to the protein (Figure 9b), again suggesting that it is a critical factor that has a dominant effect on the ΔG of folding.

As an experimental check of this prediction that flexibility permitting the folded state distance to occur is critical, the very flexible linker **3** was synthesized. This linker has the same number of heavy atoms linking the attachment sites and the same general structure as linker **2** except that the rigid triple bond is replaced with a single bond (Figure 10a) (see the Supporting Information for distance distributions of free linker **3**). Our analysis would predict that **3** would not substantially destabilize the folded state in *cis* or *trans* forms, because it can readily assume distances compatible with the folded state in both isomeric forms (Table 2).

As expected, the ^{19}F NMR spectra of the **3**-cross-linked species (Figure 10b, Table 2) show a large fraction of folded state (although somewhat smaller than that of the un-cross-linked form), and this does not change upon irradiation. This result is supported by circular dichroism spectra that indicate there is no change in secondary structure upon irradiation (Figure 10c). Thus, linker flexibility that permits Cα−Cα (or S−S) distances compatible with those of the folded state must be scrupulously avoided if effective photocontrol is desired.

Finally, we asked what role protein flexibility may play. That is, although a particular range of distances between sites 3 and

dx.doi.org/10.1021/bi300685a | *Biochemistry* 2012, 51, 6421−6431

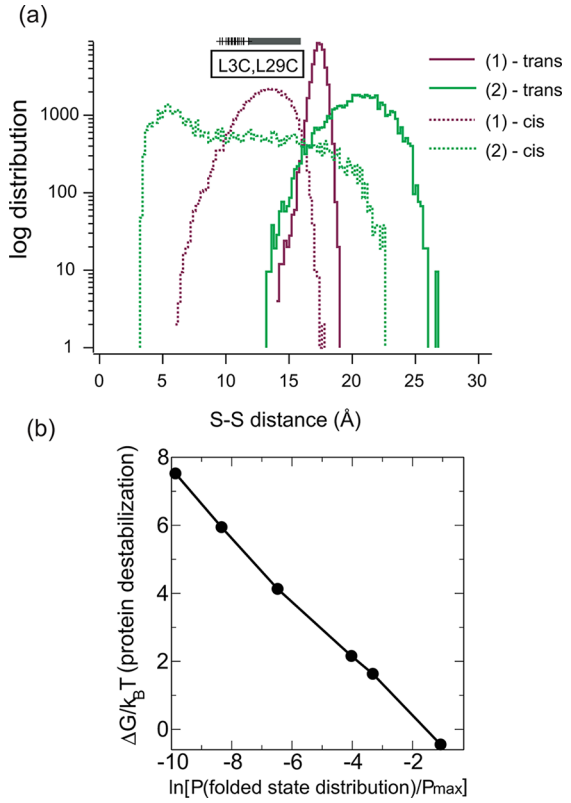

Figure 9. (a) Log histograms showing the sulfur-to-sulfur distance distributions of the isolated cross-linkers (after reaction with a Cys residue at each end, as in Figure 1). Note that cross-linker **2** samples distances compatible with the folded state L3C/L29C distance more frequently than linker **1**. (b) Plot of the model free energy of protein destabilization vs the logarithm of the ratio between the model free linker population at the folded state distance and the peak population P_{max} in the same free linker end-to-end distance distribution. Results are shown for the series of model *trans* linkers in Figure 5f with θ_0 = 104.5° and k_θ = 0, 1.5, 2.0, 4.0, 6.0, and 8.0 (see also Figure S12a of the Supporting Information). The corresponding log histograms of model free linker end-to-end distance distributions are provided in Figure S13 of the Supporting Information.

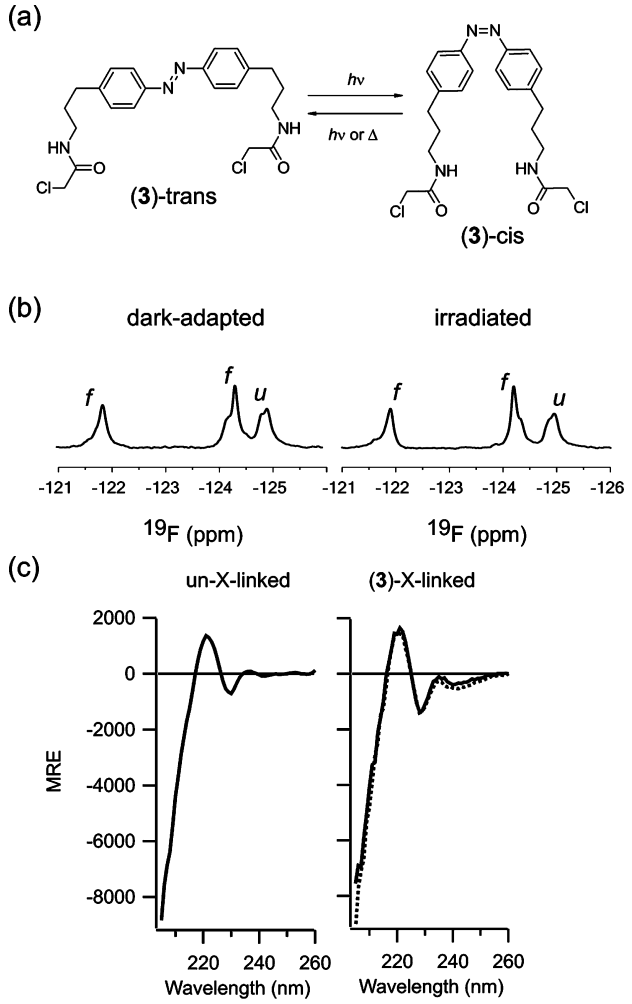

Figure 10. (a) Chemical structure of the flexible linker (**3**). For synthesis, see the Supporting Information. (b) ^{19}F NMR spectra of 5-F-Trp-labeled 3-cross-linked L3C/L29C Fyn SH3 at 20 °C under dark-adapted conditions (left) and after UV irradiation (right). (c) CD of un-cross-linked L3C/L29C Fyn SH3 at 20 °C (left) and **3**-cross-linked (right) before (—) and after (···) UV irradiation.

29 is observed in the native folded state (Figure 1), could local distortion of the protein structure allow longer values for r_{3-29} without a significant loss of the total number of native contacts? The modeling provides some insight into this question. Figure 8c plots r_{3-29} distributions for the subset of protein conformations with high values of Q (most native contacts are intact). As cross-linker stiffness increases (i.e., as r_{3-29} corresponding to the native folded state is disfavored), a population of protein conformations with specific nonnative r_{3-29} accumulates (indicated by the arrow in Figure 8c). Figure 11 shows representative structures belonging to this population.

Such partially misfolded conformations may interconvert with normally folded states and lead to the dynamic behavior observed in the HSQC spectra of **2**-cross-linked protein (Figures 2c and 3e,f). It is not clear why the short linker does not seem to produce this misfolding but seems only to promote unfolding. Perhaps the very narrow distance range permitted by the short linker allows only the native state or an open unfolded state but does not allow specific partially misfolded conformations to be significantly populated.

Outlook for the Design of Photoswitchable Proteins. This work provides some clear guidelines for designing photocontrolled proteins using intramolecular cross-linkers. For the Fyn SH3 domain, as for many proteins, function is connected with binding to a ligand (in the SH3 case, the ligand is another protein). Our guiding assumption is that photocontrol of function may be achieved by disrupting the native folded state and thereby destroying the ligand binding interface.

First, our results indicate that the greatest degree of destabilization of the native state will be afforded by long, rigid cross-linkers and any flexibility that permits distances near the normally folded state distance will be deleterious. Second, cross-linkers can cause changes in protein dynamics, perhaps through making misfolded states accessible. Although altered

Table 2. Characterization of 3-Linked Protein

protein	fraction folded (*trans*)	$\Delta G/k_BT$ (*trans*)	$\Delta G/k_BT$ (relative to un-cross-linked)[a]	fraction folded (irradiated)[b]
un-cross-linked	0.92	−2.4	0	0.92
3-cross-linked	0.72	−0.95	1.45	0.75

[a]See the text for details. [b]Not corrected for % *cis*.

dx.doi.org/10.1021/bi300685a | *Biochemistry* 2012, 51, 6421−6431

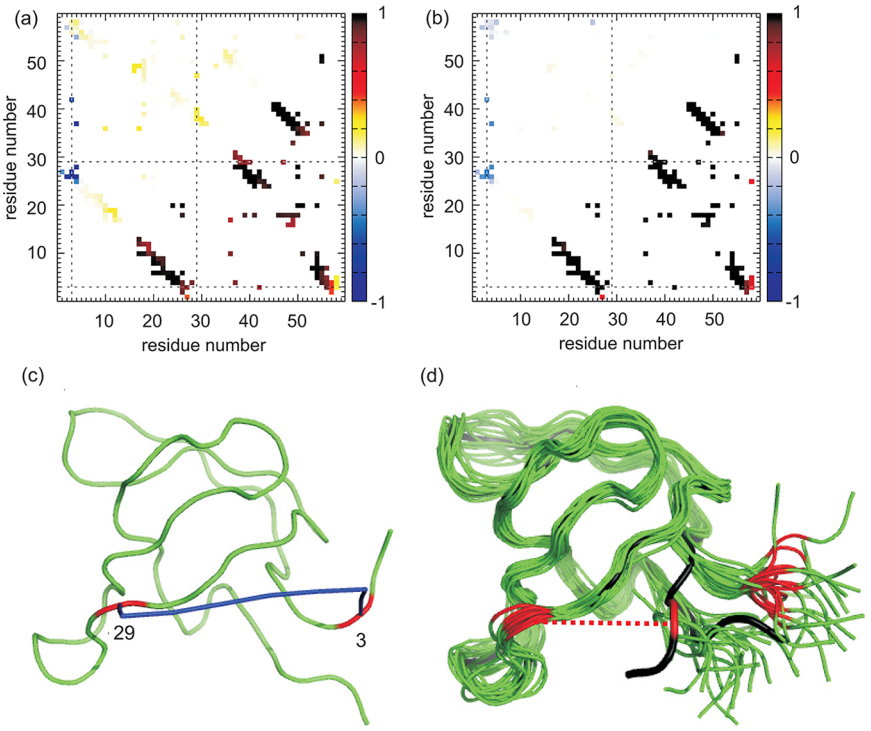

Figure 11. *Trans* linkers can induce a partially misfolded state. Probabilities of pairwise native contacts in our model protein were determined at the same simulation temperature as that used for Figure 6b. Sampling was conducted in the presence and absence of the *trans* linker with $\theta_0 = 104.5°$ and $k_\theta = 8$. Native contact probability maps are shown for conformations with (a) $0.87 < Q < 0.9$ and (b) $Q > 0.87$. The bottom right maps provide the contact probabilities for the WT (un-cross-linked) model protein, whereas the top left maps provide the differences in contact probability between the cross-linked and un-cross-linked model protein (former minus latter). The dashed lines mark the positions of the cross-linked residues. The blue spots [negative differences (see the color code at the right)] in the top left maps indicate reduced probabilities for contacts involving residues around position 3, especially those between residues around positions 3 and 29. (c) Shown here is a snapshot of the model protein (green) in a partially unfolded conformation with the model *trans* linker (blue) cross-linking positions 3 and 29 (red). (d) Ensemble of partially unfolded conformations. The black trace is the PDB structure. The green traces depict 20 randomly selected conformations with $Q > 0.87$ and $r_{3-29} > 18$. Positions 3 and 29 are colored red. The red dashed line indicates the approximate distance between these two residues in the PDB structure. It is clear from this drawing that the *trans* linker pushes position 3 significantly to the right. The Cα traces in this figure were generated using PyMOL.

dynamics can sometimes alter protein function,[56] in other cases function is unaffected;[57,58] thus, it would seem that trying to control function by controlling dynamics would be difficult. In any case, it is not clear how cross-linker structure specifically relates to protein dynamics. Instead, it would seem better at this stage to focus on protein folding thermodynamics and particularly the loss of native contacts. Importantly, the misfolded state identified by modeling (Figure 11) that can be produced by a distance constraint between residues 3 and 29 would likely not disrupt ligand binding because all the native contacts making up the ligand binding interface are intact (Figure S1 of the Supporting Information shows a model of the Fyn SH3 domain oriented to show the ligand). Thus, cross-linking sites should be chosen so that, when constrained to have distances longer than native state distances, maximal disruption of native state contacts associated with ligand binding occurs. Cross-linking at sites 3 and 29 may not be ideal in this regard. Models of the type developed here could be used to screen possible linker attachment sites according to this criterion.

■ ASSOCIATED CONTENT

Supporting Information

Details of the synthesis of the cross-linkers, protein expression, cross-linking and purification, UV, CD, and NMR analysis and further details of the construction of the model linkers and of the protein folding simulations. This material is available free of charge via the Internet at http://pubs.acs.org.

■ AUTHOR INFORMATION

Corresponding Authors

*H.S.C.: e-mail, chan@arrhenius.med.utoronto.ca; telephone, (416) 978-2697.

*G.A.W.: e-mail, awoolley@chem.utoronto.ca; telephone, (416) 978-0675.

Author Contributions

A.A.B. and T.C. contributed equally to this work.

Funding

We would like to thank NSERC, CIHR, and the CRC program for funding. H.S.C. thanks the Canada Research Chairs Program for support. A.M.A. is a trainee in the CIHR Training Program in Protein Folding.

Notes

The authors declare no competing financial interest.

■ ACKNOWLEDGMENTS

T.C. and H.S.C. are grateful for the computing resources provided by SciNet and SHARCNET of Compute Canada.

■ ABBREVIATIONS

AMBER, Assisted Model Building with Energy Refinement; CHARMM, Chemistry at HARvard Macromolecular Mechanics; HSQC, heteronuclear single-quantum correlation; MD, molecular dynamics; PDB, Protein Data Bank; WT, wild-type.

■ REFERENCES

(1) Yao, X., Rosen, M. K., and Gardner, K. H. (2008) Estimation of the available free energy in a LOV2-J alpha photoswitch. *Nat. Chem. Biol. 4*, 491−497.

(2) Banghart, M., Borges, K., Isacoff, E., Trauner, D., and Kramer, R. H. (2004) Light-activated ion channels for remote control of neuronal firing. *Nat. Neurosci. 7*, 1381−1386.

(3) Shimizu-Sato, S., Huq, E., Tepperman, J. M., and Quail, P. H. (2002) A light-switchable gene promoter system. *Nat. Biotechnol. 20*, 1041−1044.

(4) Szobota, S., and Isacoff, E. Y. (2010) Optical control of neuronal activity. *Annu. Rev. Biophys. Biomol. Struct. 39*, 329−348.

(5) Schierling, B., Noël, A.-J., Wende, W., Hien, L. T., Volkov, E., Kubareva, E., Oretskaya, T., Kokkinidis, M., Römpp, A., Spengler, B., and Pingoud, A. (2010) Controlling the enzymatic activity of a restriction enzyme by light. *Proc. Natl. Acad. Sci. U.S.A. 107*, 1361−1366.

(6) Milanesi, L., Jelinska, C., Hunter, C. A., Hounslow, A. M., Staniforth, R. A., and Waltho, J. P. (2008) A method for the reversible trapping of proteins in non-native conformations. *Biochemistry 47*, 13620−13634.

(7) Kolano, C., Helbing, J., Kozinski, M., Sander, W., and Hamm, P. (2006) Watching hydrogen-bond dynamics in a β-turn by transient two-dimensional infrared spectroscopy. *Nature 444*, 469−472.

(8) Lu, H. S. M., Volk, M., Kholodenko, Y., Gooding, E., Hochstrasser, R. M., and DeGrado, W. F. (1997) Aminothiotyrosine disulfide, an optical trigger for initiation of protein folding. *J. Am. Chem. Soc. 119*, 7173−7180.

(9) Tucker, M. J., Courter, J. R., Chen, J. X., Atasoylu, O., Smith, A. B., and Hochstrasser, R. M. (2010) Tetrazine phototriggers: Probes for peptide dynamics. *Angew. Chem., Int. Ed. 49*, 3612−3616.

(10) Takahashi, I., Kuroiwa, S., Lindfors, H. E., Ndamba, L. A., Hiruma, Y., Yajima, T., Okishio, N., Ubbink, M., and Hirota, S. (2009) Modulation of protein-ligand interactions by photocleavage of a cyclic peptide using phosphatidylinositol 3-kinase SH3 domain as model system. *J. Pept. Sci. 15*, 411−416.

(11) Umezawa, N., Noro, Y., Ukai, K., Kato, N., and Higuchi, T. (2011) Photocontrol of peptide function: Backbone cyclization strategy with photocleavable amino acid. *ChemBioChem 12*, 1694−1698.

(12) Loudwig, S., and Bayley, H. (2005) Light-activated proteins. In *Dynamic Studies in Biology* (Goeldner, M., and Givens, R. S., Eds.) pp 253−304, Wiley-VCH Verlag GmbH & Co., Berlin.

(13) Wu, Y. I., Frey, D., Lungu, O. I., Jaehrig, A., Schlichting, I., Kuhlman, B., and Hahn, K. M. (2009) A genetically encoded photoactivatable Rac controls the motility of living cells. *Nature 461*, 104−108.

(14) Aemissegger, A., Krautler, V., van Gunsteren, W. F., and Hilvert, D. (2005) A photoinducible β-hairpin. *J. Am. Chem. Soc. 127*, 2929−2936.

(15) Beharry, A. A., and Woolley, G. A. (2011) Azobenzene photoswitches for biomolecules. *Chem. Soc. Rev. 40*, 4422−4437.

(16) Schrader, T. E., Schreier, W. J., Cordes, T., Koller, F. O., Babitzki, G., Denschlag, R., Renner, C., Loweneck, M., Dong, S. L., Moroder, L., Tavan, P., and Zinth, W. (2007) Light-triggered β-hairpin folding and unfolding. *Proc. Natl. Acad. Sci. U.S.A. 104*, 15729−15734.

(17) Burns, D. C., Flint, D. G., Kumita, J. R., Feldman, H. J., Serrano, L., Zhang, Z., Smart, O. S., and Woolley, G. A. (2004) Origins of helix-coil switching in a light-sensitive peptide. *Biochemistry 43*, 15329−15338.

(18) Woolley, G. A. (2005) Photocontrolling peptide α helices. *Acc. Chem. Res. 38*, 486−493.

(19) Zhang, F., Zarrine-Afsar, A., Al-Abdul-Wahid, M. S., Prosser, R. S., Davidson, A. R., and Woolley, G. A. (2009) Structure-based approach to the photocontrol of protein folding. *J. Am. Chem. Soc. 131*, 2283−2289.

(20) Woolley, G. A., Lee, E. S., and Zhang, F. (2006) sGAL: A computational method for finding surface exposed sites in proteins suitable for Cys-mediated cross-linking. *Bioinformatics 22*, 3101−3102.

(21) Moglich, A., and Moffat, K. (2010) Engineered photoreceptors as novel optogenetic tools. *Photochem. Photobiol. Sci. 9*, 1286−1300.

(22) Pace, C. N., Grimsley, G. R., Thomson, J. A., and Barnett, B. J. (1988) Conformational stability and activity of ribonuclease T1 with zero, one, and two intact disulfide bonds. *J. Biol. Chem. 263*, 11820−11825.

(23) Flory, P. J. (1956) Theory of elastic mechanisms in fibrous proteins. *J. Am. Chem. Soc. 78*, 5222−5234.

(24) Zhou, H. X. (2004) Polymer models of protein stability, folding, and interactions. *Biochemistry 43*, 2141−2154.

(25) Chan, H. S., Zhang, Z., Wallin, S., and Liu, Z. (2011) Cooperativity, local-nonlocal coupling, and nonnative interactions: Principles of protein folding from coarse-grained models. *Annu. Rev. Phys. Chem. 62*, 301−326.

(26) Hamacher, K., Hubsch, A., and McCammon, J. A. (2006) A minimal model for stabilization of biomolecules by hydrocarbon cross-linking. *J. Chem. Phys. 124*, 164907.

(27) Kutchukian, P. S., Yang, J. S., Verdine, G. L., and Shakhnovich, E. I. (2009) All-atom model for stabilization of α-helical structure in peptides by hydrocarbon staples. *J. Am. Chem. Soc. 131*, 4622−4627.

(28) Ihalainen, J. A., Paoli, B., Muff, S., Backus, E. H., Bredenbeck, J., Woolley, G. A., Caflisch, A., and Hamm, P. (2008) α-Helix folding in the presence of structural constraints. *Proc. Natl. Acad. Sci. U.S.A. 105*, 9588−9593.

(29) Cutler, T. A., Mills, B. M., Lubin, D. J., Chong, L. T., and Loh, S. N. (2009) Effect of Interdomain Linker Length on an Antagonistic Folding-Unfolding Equilibrium between Two Protein Domains. *J. Mol. Biol. 386*, 854−868.

(30) Shea, J. E., Onuchic, J. N., and Brooks, C. L. (1999) Exploring the origins of topological frustration: Design of a minimally frustrated model of fragment B of protein A. *Proc. Natl. Acad. Sci. U.S.A. 96*, 12512−12517.

(31) Clementi, C., Nymeyer, H., and Onuchic, J. N. (2000) Topological and energetic factors: What determines the structural details of the transition state ensemble and "en-route" intermediates for protein folding? An investigation for small globular proteins. *J. Mol. Biol. 298*, 937−953.

(32) Koga, N., and Takada, S. (2001) Roles of native topology and chain-length scaling in protein folding: A simulation study with a Go-like model. *J. Mol. Biol. 313*, 171−180.

(33) Dokholyan, N. V., Li, L., Ding, F., and Shakhnovich, E. I. (2002) Topological determinants of protein folding. *Proc. Natl. Acad. Sci. U.S.A. 99*, 8637−8641.

(34) Kaya, H., and Chan, H. S. (2003) Solvation effects and driving forces for protein thermodynamic and kinetic cooperativity: How adequate is native-centric topological modeling? *J. Mol. Biol. 326*, 911−931. (2004) *337*, 1069−1070 (Corrigendum).

(35) Weikl, T. R., and Dill, K. A. (2003) Folding kinetics of two-state proteins: Effect of circularization, permutation, and crosslinks. *J. Mol. Biol. 332*, 953−963.

(36) Zarrine-Afsar, A., Wallin, S., Neculai, A. M., Neudecker, P., Howell, P. L., Davidson, A. R., and Chan, H. S. (2008) Theoretical and experimental demonstration of the importance of specific nonnative interactions in protein folding. *Proc. Natl. Acad. Sci. U.S.A. 105*, 9999−10004.

(37) Zhang, Z., and Chan, H. S. (2010) Competition between native topology and nonnative interactions in simple and complex folding kinetics of natural and designed proteins. *Proc. Natl. Acad. Sci. U.S.A. 107*, 2920−2925.

(38) Zarrine-Afsar, A., Zhang, Z., Schweiker, K. L., Makhatadze, G. I., Davidson, A. R., and Chan, H. S. (2012) Kinetic consequences of

native state optimization of surface-exposed electrostatic interactions in the Fyn SH3 domain. *Proteins 80*, 858−870.
(39) Rau, H. (1990) Photoisomerization of azobenzenes. In *Photochemistry and Photophysics* (Rabek, J. F., Ed.) pp 119−141, CRC Press Inc., Boca Raton, FL.
(40) Dias, A. R., Minas da Piedade, M. E., Martinho Simoes, J. A., Simoni, J. A., Teixeira, C., Diogo, H. P., Meng-Yan, Y., and Pilcher, G. (1992) Enthalpies of formation of cis-azobenzene and trans azobenzene. *J. Chem. Thermodyn. 24*, 439−447.
(41) Rose, G. D., Fleming, P. J., Banavar, J. R., and Maritan, A. (2006) A backbone-based theory of protein folding. *Proc. Natl. Acad. Sci. U.S.A. 103*, 16623−16633.
(42) Korzhnev, D. M., Salvatella, X., Vendruscolo, M., Di Nardo, A. A., Davidson, A. R., Dobson, C. M., and Kay, L. E. (2004) Low-populated folding intermediates of Fyn SH3 characterized by relaxation dispersion NMR. *Nature 430*, 586−590.
(43) Plaxco, K. W., Guijarro, J. I., Morton, C. J., Pitkeathly, M., Campbell, I. D., and Dobson, C. M. (1998) The folding kinetics and thermodynamics of the Fyn-SH3 domain. *Biochemistry 37*, 2529−2537.
(44) Larson, S. M., and Davidson, A. R. (2000) The identification of conserved interactions within the SH3 domain by alignment of sequences and structures. *Protein Sci. 9*, 2170−2180.
(45) Chi, L., Sadovski, O., and Woolley, G. A. (2006) A blue-green absorbing cross-linker for rapid photoswitching of peptide helix content. *Bioconjugate Chem. 17*, 670−676.
(46) Zhang, F., Sadovski, O., and Woolley, G. A. (2008) Synthesis and characterization of a long, rigid photoswitchable cross-linker for promoting peptide and protein conformational change. *ChemBioChem 9*, 2147−2154.
(47) Tsodikov, O. V., Record, M. T., Jr., and Sergeev, Y. V. (2002) Novel computer program for fast exact calculation of accessible and molecular surface areas and average surface curvature. *J. Comput. Chem. 23*, 600−609.
(48) Liu, Z. R., and Chan, H. S. (2005) Solvation and desolvation effects in protein folding: Native flexibility, kinetic cooperativity and enthalpic barriers under isostability conditions. *Phys. Biol. 2*, S75−S85.
(49) Liu, Z. R., and Chan, H. S. (2005) Desolvation is a likely origin of robust enthalpic barriers to protein folding. *J. Mol. Biol. 349*, 872−889.
(50) Cheung, M. S., Garcia, A. E., and Onuchic, J. N. (2002) Protein folding mediated by solvation: Water expulsion and formation of the hydrophobic core occur after the structural collapse. *Proc. Natl. Acad. Sci. U.S.A. 99*, 685−690.
(51) Klimov, D. K., and Thirumalai, D. (2002) Stiffness of the distal loop restricts the structural heterogeneity of the transition state ensemble in SH3 domains. *J. Mol. Biol. 317*, 721−737.
(52) Ollerenshaw, J. E., Kaya, H., Chan, H. S., and Kay, L. E. (2004) Sparsely populated folding intermediates of the Fyn SH3 domain: Matching native-centric essential dynamics and experiment. *Proc. Natl. Acad. Sci. U.S.A. 101*, 14748−14753.
(53) Sugita, Y., Kitao, A., and Okamoto, Y. (2000) Multidimensional replica-exchange method for free-energy calculations. *J. Chem. Phys. 113*, 6042−6051.
(54) Murata, K., Sugita, Y., and Okamoto, Y. (2004) Free energy calculations for DNA base stacking by replica-exchange umbrella sampling. *Chem. Phys. Lett. 385*, 1−7.
(55) Badasyan, A., Liu, Z. R., and Chan, H. S. (2008) Probing possible downhill folding: Native contact topology likely places a significant constraint on the folding cooperativity of proteins with similar to 40 residues. *J. Mol. Biol. 384*, 512−530.
(56) Karplus, M., and Kuriyan, J. (2005) Molecular dynamics and protein function. *Proc. Natl. Acad. Sci. U.S.A. 102*, 6679−6685.
(57) Doucet, N., Khirich, G., Kovrigin, E. L., and Loria, J. P. (2011) Alteration of hydrogen bonding in the vicinity of histidine 48 disrupts millisecond motions in RNase A. *Biochemistry 50*, 1723−1730.
(58) Doucet, N. (2011) Can enzyme engineering benefit from the modulation of protein motions? Lessons learned from NMR relaxation dispersion experiments. *Protein Pept. Lett. 18*, 336−343.